

# Efficient Self-Ensemble Framework for Semantic Segmentation

Walid Bousselham

Guillaume Thibault

Lucas Pagano

Archana Machireddy

Joe Gray

Young Hwan Chang

Xubo Song

Oregon Health and Science University  
Portland, OR, USA

## Abstract

*Ensemble of predictions is known to perform better than individual predictions taken separately. However, for tasks that require heavy computational resources, e.g. semantic segmentation, creating an ensemble of learners that needs to be trained separately is hardly tractable. In this work, we propose to leverage the performance boost offered by ensemble methods to enhance the semantic segmentation, while avoiding the traditional heavy training cost of the ensemble. Our self-ensemble framework takes advantage of the multi-scale features set produced by feature pyramid network methods to feed independent decoders, thus creating an ensemble within a single model. Similar to the ensemble, the final prediction is the aggregation of the prediction made by each learner. In contrast to previous works, our model can be trained end-to-end, alleviating the traditional cumbersome multi-stage training of ensembles. Our self-ensemble framework outperforms the current state-of-the-art on the benchmark datasets ADE20K, Pascal Context and COCO-Stuff-10K for semantic segmentation and is competitive on Cityscapes. Code will be available at [github.com/WalBouss/SenFormer](https://github.com/WalBouss/SenFormer).*

## 1. Introduction

Semantic segmentation is the task of assigning each pixel of an image with a semantic category, and therefore is close to the task of image classification. Its many applications include robotics, autonomous cars, medical application, augmented reality and more. Most segmentation methods follow an Encoder-Decoder scheme. The encoder extracts the relevant features of the image to characterize each pixel, a process usually involving down-sampling the feature maps to increase the receptive field of the model. The decoder up-samples the feature maps to both recover the spatial in-

formation and produce a per-pixel classification. In [31] the authors extended this procedure to fully convolutional network (FCN), which paved the way for later work to achieve impressive results on various segmentation datasets and has since dominated the field of semantic segmentation, let it be for medical [19,38], self-driving cars [40] or robotics applications [20].

While for image classification all the extracted features are aggregated to generate a single prediction for the whole image, for semantic segmentation one prediction is made per pixel, and therefore, each location within a given feature map needs to contain information about its own class and the class of its surroundings. Research efforts have focused on enhancing FCN, mainly to compensate for the inherent locality of the convolution operation. Some examples of convolution enhancements for segmentation are the atrous convolution that introduces holes in convolution kernel [6,7], the pyramid pooling module (PPM) that aggregates context information using different kernel pooling layers, and [48] that combine the PPM and the feature pyramid network (FPN) [27] to capture context information at different resolutions. The level of efforts to circumvent convolution locality reflects its limitation for semantic segmentation.

Following the hegemony of transformer-based architectures over natural language processing (NLP) tasks, much attention has been given to transformer-based network in vision applications. Since Dosovitskiy *et al.* introduced the Vision Transformer (ViT) [12] and Touvron *et al.* [42] an efficient training strategy, a series of transformer-based backbone have been developed [13,30,45,46], tending towards replacing their convolution counterparts. Recently, semantic segmentation has been reformulated as a sequence-to-sequence prediction problem, and has resulted in state of the art results [9,41,44,49,53].

Another promising line of improvement, though not

widely explored, is the use of ensemble methods which combines predictions from multiple learners. Modern deep learning architectures rely on stochastic optimizers for training (*e.g.* SGD). They are highly sensitive to initialization, choices of hyper-parameters, and data augmentation, and, as a result, tend to converge to different local minimum and thus yield different predictions [15]. However, by training multiple models separately and averaging their predictions, it is possible to reduce the prediction variance and generate performances that are better than any individual model. While ensemble learning has been extensively applied to classification [24, 33, 50], deep metric learning [23, 25], and to some extent to object detection [1, 47], its application to semantic segmentation [34, 37] is still limited, mainly due to the prohibitive cost of model training.

We propose a simple transformer-based decoder that can be interpreted as **Self-ensemble segmentation transFormer (SenFormer)**. To take advantage of the performance boost brought by ensemble methods while avoiding the inconvenience and cost of training several models, we propose to leverage the multi-scale feature pyramid naturally produced by the FPN-like methods, by feeding independent decoders with the aim to constitute an ensemble of learners, which can be interpreted as a form of self-ensemble segmentation. Since the inputs to the learners (*i.e.* decoders) come from different levels of the feature pyramid, they differ in scale and contain different spatial and semantic information, allowing each learner to make prediction that is inherently different from others. Such diversity introduced between the learners has been known to increase the performance in ensemble learning [55]. It has been reported that when the learners are trained with a loss function on the final merged decision, the boost in performance offered by ensemble is not observed [2]. However, our experiments indicate that it is not the case in our self-ensemble framework. After conducting extensive ablation studies, we further demonstrate that the benefits of our method effectively come from the self-ensemble framework by comparing the SenFormer to a custom baseline that uses a features fusion strategy.

Overall, our SenFormer approach achieves excellent results on benchmark datasets. Specifically, it outperforms similar architectures [48] that use feature fusion strategy, suggesting that our self-ensemble approach effectively leverage the expressive power of ensemble methods. In particular, when using a larger backbone model, SenFormer achieves an accuracy of 57.05% on the benchmark ADE20k data set [54], outperforming the current state-of-the-art of 56.7% [3]. To summarize, our contributions are three fold:

- We propose an innovative way to leverage the multi-scale features produced by the FPN to form an ensemble of learners inside a single model.
- We develop a transformer-based decoder that is used

as a learner in our self-ensemble framework.

- We propose an enhancement of the traditional FPN that uses transformer blocks in place of convolutions.

## 2. Related Works

**Semantic Segmentation.** Since fully convolutional networks (FCN) have been introduced in the seminal work [31], it has dominated the field of semantic segmentation. However, due to the inherent locality of the convolution operation, architectures solely based on convolutions fail to capture long-range dependencies and thus prevent it from capturing global context information, which is vital for dealing with large and/or occluded objects. To alleviate the locality issue innate to convolution, a series of enhancements have been introduced to the FCN scheme. In [6, 7], *atrous convolution* was introduced to increase the convolution receptive field by introducing holes in the convolution kernel. In [52], it was acknowledged that due to the limited access to context information, FCN mainly based its prediction on the shape of the object of interest, rather than on the scene context. This led to the proposed Pyramid Scene Parsing Network (PSPNet) and the introduction of a *pyramid pooling module* (PPM) that consists of a series of pooling layers with different kernel sizes, processed in parallel and then concatenated before feeding to the decoder. Although PPM allows the aggregation of more context information, the PSPNet decoder in [52] used only low-resolution feature maps for segmentation and lacked spatial information in the decoder. In addition to using PPM, to obtain feature maps that were more spatially aware, a feature pyramid network (FPN) was used in [48], which were concatenated with PPM output for segmentation prediction.

**Vision Transformers.** More recently, motivated by the stupendous success of transformer-based architecture for image classification [12, 42], there have been several works leveraging the self-attention operation to improve segmentation performance of FCN scheme or even completely replacing it. Transformer-based architectures can be used as a drop-in replacement of traditional CNN backbones to enhance the extracted features supplied to the decoder [13, 30, 42, 45, 46]. It has been observed that transformer backbones that produce a hierarchical feature representation [30, 45] are the most suited for segmentation tasks. Additionally, following the original Encoder-Decoder Transformer [43] used in NLP, recent works proposed to formulate the problem of semantic segmentation as a sequence-to-sequence problem [41, 49, 53], freeing the architecture from any inductive prior biases.

Alternatively, motivated by the success of DETR [5] which used transformer for object detection, MaX-DeepLab [44] and MaskFormer [9] treated semantic (and panoptic) segmentation no longer as a per-pixel classification but as a

mask classification problem.

These architectures first generate a set of candidate masks that are then classified. While shifting the semantic segmentation paradigm from a per-pixel classification to a mask classification problem helps to bridge the gap between detection/panoptic segmentation methods and semantic segmentation, it also involves the computation of an assignment score between each generated mask and every class, therefore transferring a part of the training burden to the loss calculation. Since our focus is on investigating the efficacy of features fusion and self-ensemble, we will limit our comparisons to per-pixel classification-based architectures.

### 3. Method

In this section, we describe how the multi-scale feature pyramid is generated by the FPN and present our proposed version, which we call the feature pyramid network transformer (FPNT). Then, we introduce the transformer-based decoder architecture used in this paper. Finally, we describe our overall self-ensemble framework (Figure 1) to improve segmentation models.

#### 3.1. Multi-scale feature extraction

##### 3.1.1 Notations

Following the notations in [18, 27, 48], we denote the output of the last residual block of ResNet-like backbones as  $\{C_2, C_3, C_4, C_5\}$  with respective strides of  $\{4, 8, 16, 32\}$ . For Swin Transformer-like backbones,  $\{C_2, C_3, C_4, C_5\}$  correspond to the output of stage 1 up to stage 4 that also have respective stride of  $\{4, 8, 16, 32\}$ , see Figure 1.

##### 3.1.2 Feature Pyramid Network

The set of features extracted by the backbone is enhanced by the FPN [27] to obtain a feature pyramid that has strong spatial and semantics at all scales. To do so,  $\{C_2, C_3, C_4, C_5\}$  undergo a linear projection to set the channel dimension of each scale to a fixed size denoted as  $D$ . Consecutive levels are then upsampled to the same size (through bilinear interpolation) and merged by element-wise addition. Eventually, the merged features are processed by a  $3 \times 3$  convolution to alleviate the aliasing effect of the upsampling (see [27] for more details). We denote the FPN feature set output as  $\mathcal{P} = \{P_2, P_3, P_4, P_5\}$ , where

$$\begin{aligned} P'_i &= Proj(C_i), \quad i \in \{2, 3, 4, 5\} \\ P_5 &= P'_5 \\ P_i &= Conv_{3 \times 3}(P'_i + Upsample(P'_{i+1})), \quad i \in \{2, 3, 4\} \end{aligned} \quad (1)$$

with  $Conv_{3 \times 3}$  being a convolution with  $3 \times 3$  kernel and  $Upsample$  being the nearest neighbor upsampling operation.

#### 3.1.3 Feature Pyramid Network Transformer

We empirically found that while introducing marginal changes to the implementation and a minimal computational cost, replacing the  $3 \times 3$  convolution by a *transformer block* in the FPN increases the segmentation performance (see ablation studies Section 4.4). In practice, we use the window-based transformer block (denoted as WTB) of [30] to limit the memory footprint overhead. We name this enhanced FPN version as feature pyramid network transformer (FPNT), where

$$\begin{aligned} P'_i &= Proj(C_i), \quad i \in \{2, 3, 4, 5\} \\ P_5 &= P'_5 \\ P_i &= WTB(P'_i + Upsample(P'_{i+1})), \quad i \in \{2, 3, 4\} \end{aligned} \quad (2)$$

#### 3.2. Decoders architecture

In this paper, the problem of semantic segmentation is approached as a per-pixel classification through ensemble learning. This means that the final class assignment prediction for each pixel is not the output of a single decoder, but rather the fused predictions made by different independent learners. Hereafter, we described the architecture of a single decoder and in the next section we present our self-ensemble framework.

**Transformer Decoders.** As depicted in Figure 1, the  $i^{th}$  decoder branch takes as input the features coming from the corresponding level of the FPN (with stride  $s_i$ )  $P_i \in \mathcal{R}^{D \times \frac{H}{s_i} \times \frac{W}{s_i}}$ , as well as a set of  $N_c$  learnable embeddings termed as class embeddings,  $\mathbf{cls}_i = [cls_i^1, \dots, cls_i^{N_c}] \in \mathcal{R}^{N_c \times D}$ , where  $N_c$  is the number of class. In this respect, there is one learnable class embedding  $cls_i^k$  per segmentation class and per level in the feature pyramid.

Each decoder is a transformer composed of  $L$  layers whose architecture is inspired by the traditional transformer [43], except that we do not use any encoder layers, plus we use pre-norm in place of post-norm for the placement of *layer normalization* (LN), meaning that the skip connections inside each transformer block are not affected by the LN [36].

In a nutshell, a single Transformer Decoder block consists of three successive operations: *Cross-Attention*, *Self-Attention* and *Multi-Layer Perceptron* layers.

First, the multi-scale features  $\{P_2, P_3, P_4, P_5\}$  are reshaped into a set of tokens  $\{z_2, z_3, z_4, z_5\}$  where  $z_i \in \mathcal{R}^{n_i \times D}$ ,  $n_i = \frac{HW}{s_i}$  is the number of token, and  $s_i$  is the stride of the  $i^{th}$  level of the pyramid.

In the **CA** layer, the FPN’s token features  $z_i$ ’s are linearly transformed through matrix multiplication to acts as the *keys* and *values*, and the class embedding  $\mathbf{cls}_i$ ’s as the

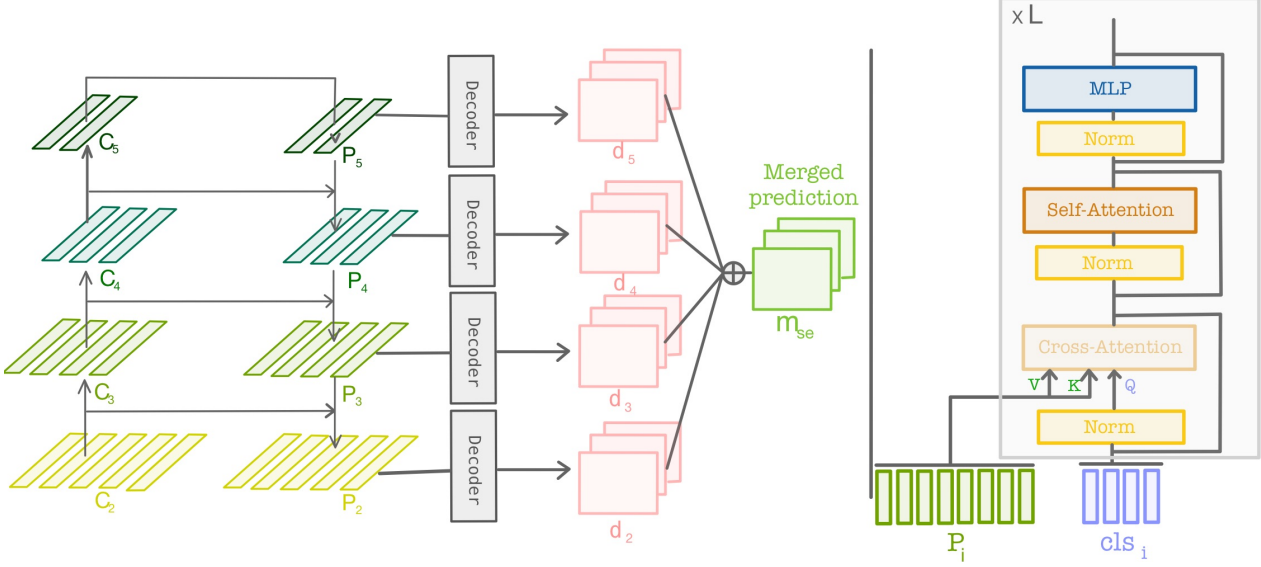


Figure 1. **SenFormer architecture.** The features extracted by the backbone  $\{C_2, C_3, C_4, C_5\}$  are enhanced in a feature pyramid to produce spatially and semantically strong features maps at every level of the pyramid. Each set of features is decoded by a different learner in the ensemble and the learners' predictions are merged.

queries. For  $i \in \{2, 3, 4, 5\}$  the CA operation is as follows:

$$\begin{aligned}
 K &= z_i W_K, V = z_i W_V, Q = \mathbf{cls}_i W_Q, \\
 \text{where } W_K, W_V, W_Q &\in \mathcal{R}^{D \times D} \\
 CA(Q_i, P_i) &= \mathbf{cls}_i + \text{softmax}\left(\frac{QK^T}{\sqrt{D}}\right)V
 \end{aligned} \tag{3}$$

where *softmax* denotes the softmax function applied along the last dimension.

This operation aims at distilling the knowledge gained by the backbone contained in the features  $P_i$ 's into the class embeddings  $\mathbf{cls}_i$ . This way the model will retain the information of *what is it for a feature token  $z_i$  to represent a specific class*. Indeed, since the class embedding vector is used to get the final prediction via a dot product with the features tokens, during the back-propagation the class embedding tensor  $cls_i^k$  (that represents the  $k^{th}$  class) will be encouraged to become similar to the tokens of  $z_i$  that correspond to the  $k^{th}$  class, according to the ground truth segmentation maps.

Then, the Self-Attention layer enables sharing the information acquired during the Cross-Attention across the class embedding vectors. Eventually, an **MLP** layer is used to propagate the information across the channel dimensions.

Overall, each decoder is composed of  $L$  layers of decoder blocks and its prediction is obtained via a dot product between the class embeddings  $\mathbf{cls}_i$  and the corresponding feature pyramid feature  $P_i$ .

### 3.3. Ensemble Prediction

#### 3.3.1 Traditional Ensemble

Traditionally, an ensemble  $\mathcal{M}^{trad}$  is a set of  $M$  *independently* trained models, denoted as  $\mathcal{M}^{trad} = \{f_1, f_2, \dots, f_M\}$  that we call learners. Each learner  $f_m$ ,  $m \leq M$  produces its own prediction for the given task that is then merged to the others to generate the final prediction. For semantic segmentation, let  $f_m^{ij} \in \mathcal{R}^{N_c}$  represent the classification prediction made by the  $m^{th}$  learner at pixel location  $(i, j)$  for a  $N_c$ -clas segmentation problem. Given an input image  $x \in \mathcal{R}^{3 \times H \times W}$ , the final ensemble segmentation mask prediction  $m(x) \in \mathcal{R}^{N_c \times H \times W}$  at location  $(i, j) \in \{1, \dots, H\} \times \{1, \dots, W\}$  is

$$m(x)^{ij} = \frac{1}{M} \sum_{m=1}^M f_m^{ij}(x) \in \mathcal{R}^{N_c} \tag{4}$$

#### 3.3.2 Self-Ensemble

In our self-ensemble setting, we have an ensemble  $\mathcal{D} = \{d_2, d_3 \dots, d_M\}$  of  $M-1$  independent learners/decoders, where  $M$  is the level index in the FPN<sup>1</sup>. The different learners do not receive the same input. Indeed, the learners share the same backbone but receive features coming from different levels of the feature pyramid.

Given an input image  $x \in \mathcal{R}^{3 \times H \times W}$ , the final self-ensemble segmentation mask prediction  $m_{se}(x) \in$

<sup>1</sup>Typically  $M = 5$ , but it can be more as in the case of RetinaNet [28].

$\mathcal{R}^{N_c \times H \times W}$  at location  $(i, j) \in \{1, \dots, H\} \times \{1, \dots, W\}$  is

$$m_{se}^{ij}(x) = \frac{1}{M-1} \sum_{m=2}^M d_m^{ij}(P_m) \in \mathcal{R}^{N_c} \quad (5)$$

where  $d_m^{ij} \in \mathcal{R}^{N_c}$  represent the classification prediction made by the  $m^{th}$  decoder at pixel location  $(i, j)$ .

Traditionally in ensembles, if one trains the different learners altogether (*i.e.*, applying the loss on the merged prediction), the performance boost offered by ensemble disappear [2]. However, our experiments show that it is not the case in our setting. We hypothesis that it is due to fact that each learners are independently initialized (as in ensemble) and receives different inputs, therefore alleviating the need for separate training.

## 4. Experiments

**Datasets.** We evaluate our model performance using four semantic segmentation benchmark datasets, ADE20K [54], Pascal Context [35], COCO-Stuff-10K [4] and Cityscapes [11]. We focus on ADE20k, which is a challenging scene parsing dataset consisting of 20,210 training images and 2,000 validation images and covers 150 fine-grained labeled classes. Results on additional datasets can be found in the supplementary materials.

**Evaluation metric.** We report the mean Intersection over Union (mIoU), a standard metric for semantic segmentation.

**Baseline model.** To demonstrate that the performance improvement of our method is genuinely a result of self-ensemble instead of feature fusion, we introduce a simple decoder baseline module that borrows the feature fusion strategy from UperNet [48], but uses our transformer decoder, as shown in Figure 2. This way, the FeatureFusion-Baseline and SenFormer only differ by the multi-scale fusion strategy. Following [48], the baseline multi-scale fusion strategy is as follow: we first resize (through bilinear interpolation) all the features  $\{P_2, P_3, P_4, P_5\}$  to match  $P_2$  dimension (*i.e.*  $1/4$  of the input image) and concatenate them. We then apply a  $3 \times 3$  convolution followed by a batch normalization layer and a ReLU activation. Note that this baseline is only used for ablation purposes and SenFormer is thereafter also compared to state of the art methods in Section 4.3.

### 4.1. Implementation and training details

**Backbones.** Since SenFormer uses the FPN to build a multi-scale set of features, it is compatible with any backbone architecture. In our experiments we use both convolutional ResNet50 and ResNet101 [18]. For transformer-based backbones, we use Swin-Transformers [30] and BEiT [3].

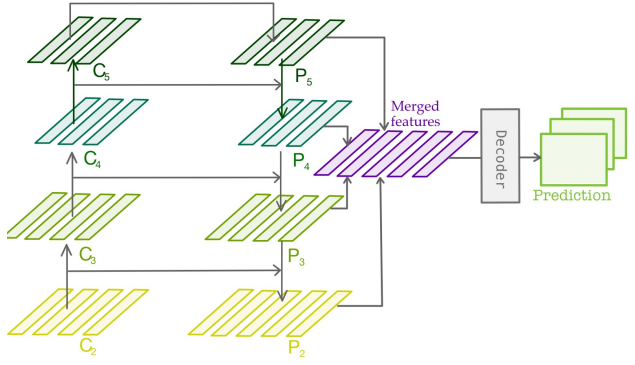


Figure 2. FeaturesFusionBaseline architecture.

**FPN and FPNT.** The channel dimension of the feature pyramid  $D$  is set to 512 for both FPN and FPNT. For the Window-based Transformer Block (WTB) of our FPNT, we follow the standard settings of [30], with a window size of  $7 \times 7$ , 8 attention heads and MLP dimension of  $4D$ .

**Transformer decoder ensemble.** SenFormer is composed of an ensemble of decoders that all share the same transformer architecture, but receive their input feature maps from different levels of the feature pyramid. Each decoder is a succession of  $L$  transformer blocks composed of a sequence of cross-attention, self-attention and a multi-layer perceptron operations, enhanced with skip-connections and pre-norm layer normalization. The number of class embedding  $\mathbf{cls}_i = [cls_i^1, \dots, cls_i^{N_c}] \in \mathcal{R}^{N_c \times D}$  for each decoder  $i$  in the ensemble is equal to  $N_c$ , the number of classes in the training dataset. Similar to [5, 9], the class embeddings are initialized to zero.

Each learner is independently supervised with a cross-entropy loss. In addition, we apply a standard cross-entropy loss on the final ensemble prediction. To sum it all up, the final loss function is,  $\mathcal{L}(x, m^{gt}) = \mathcal{L}_{ce}(m_{se}(x)) + \sum_{m=2}^5 \mathcal{L}_{ce}(d_m(P_m), m^{gt})$ .

**Training setting.** We use mmsegmentation [10] library as codebase and follow the standard training practice for each dataset. Moreover, we apply common data augmentation for semantic segmentation, which include left-right flipping, standard random color jittering, random resize with ratio  $0.5 - 2$  and random cropping.

For the optimizer, we use AdamW [32]. Following [6] in segmentation and as common practice, we use "poly" learning rate scheduler. Following [9, 48], we set the initial learning rate to  $10^{-4}$  and weight decay to  $10^{-4}$  for ResNet backbones, an initial learning rate of  $6 \cdot 10^{-6}$  and a weight decay of  $10^{-2}$  for Swin-Transformer, and an initial learning rate of  $2 \cdot 10^{-5}$  and a weight decay of 0.05 for BEiT. Due to memory limitations, no learner is used for  $P_5$  when BEiT-L is used as backbone, resulting in 3 learners instead of 4. We also use gradient clipping of 1 to help stabilizing the

	method	backbone	crop size	#params.	FLOPs	<i>mIoU</i>
CNN	UperNet	ResNet-50	512×512	<b>67M</b>	238G	42.05
	SenFormer	ResNet-50	512×512	144M	<b>179G</b>	<b>44.68</b>
	UperNet	ResNet-101	512×512	<b>86M</b>	257G	43.82
	SenFormer	ResNet-101	512×512	163M	<b>199G</b>	<b>46.54</b>
Transformer	UperNet	Swin-T	512×512	60M	236G	44.41
	SenFormer	Swin-T	512×512	144M	179G	<b>46.0</b>
	UperNet	Swin-S	512×512	81M	259G	47.72
	SenFormer	Swin-S	512×512	165M	202G	<b>49.2</b>
	UperNet	Swin-B <sup>‡</sup>	640×640	121M	471G	50.04
	SenFormer	Swin-B <sup>‡</sup>	640×640	204M	242G	<b>51.75</b>
	UperNet	Swin-L <sup>‡</sup>	640×640	234M	647G	52.05
	SenFormer	Swin-L <sup>‡</sup>	640×640	314M	546G	<b>53.08</b>
	UperNet	BEiT-L <sup>‡</sup>	640×640	441M	1746G	56.7
	SenFormer	BEiT-L <sup>‡</sup>	640×640	525M	934G	<b>57.05</b>

Table 1. **Semantic segmentation on ADE20K validation.** Comparison of self-ensemble based SenFormer with the counterpart of features-fusion based UperNet. Result in blue indicated the new state-of-the-art. Backbones pre-trained on ImageNet-22K are marked with <sup>‡</sup>.

$d_2$	$d_3$	$d_4$	$d_5$	<i>mIoU</i>
✓	✗	✗	✗	42.31
✗	✓	✗	✗	41.87
✗	✗	✓	✗	41.84
✗	✗	✗	✓	38.11
✓	✓	✓	✗	44.55
✓	✓	✓	✓	<b>44.68</b>

Table 2. Performances by using different combinations learners, where ✓/✗ indicates whether or not the learner is used for the prediction.

training, and for ResNet backbones a learning rate multiplier of 0.1 is applied. During training, the input images are cropped to a size of 512 × 512 for ADE20K, unless stated otherwise. All the models are trained on 8 V100 GPUs with a batch size of 16 for 160k iterations. The segmentation performance is reported using single-scale inference. Finally, all the backbones are pretrained on ImageNet-1K [39] unless stated otherwise.

## 4.2. Self-ensemble

Features at different levels of the pyramid carries different scale of contextual information, and our experiments support that self-ensemble is capable of capturing and integrating such information.

We first analyze the output produced by each decoder and assess their performance. Table 2 outlines the *mIoU* scores of independent prediction of each decoder as well as for the ensemble. Notably, the ensemble *mIoU* score is +3.5 better than the mean score of the learners taken

method	<i>mIoU</i>	#params.	FLOPs
FeaturesFusionBaseline	42.44	52M	262G
SenFormer	<b>44.68</b>	144M	179G

Table 3. **Baseline vs SenFormer.** Comparison of the features fusion and self-ensemble strategy.

separately with  $\sum_{i=2}^5 mIoU(d_i) = 41.03$ . More surprisingly, even though  $d_5$  taken separately performs significantly worse than the others – due to its low-resolution inputs – when introduced in the ensemble it positively contributes to the model, thereby is consistent with traditional ensemble methods where even weak learners can be combined to enhance the prediction.

**Feature Fusion vs SenFormer.** To verify that the gain in performance of our model effectively arises self-ensemble, we compare SenFormer and the FeaturesFusionBaseline, since they only differ in the multi-scale fusion strategy (*features fusion vs self-ensemble*). In Table 3, we observe that SenFormer is +2 *mIoU* better than the baseline, suggesting that our self-ensemble approach is indeed the main drive for the improvement.

## 4.3. Main results

**Results.** The current state-of-the-art performance for pixel-based semantic segmentation on the benchmark data set ADE20K is obtained by an UperNet [48] with BEiT [3] backbone and a *features fusion* strategy, with a *mIoU* of 56.7. In our experiments, we compare SenFormer with UperNet architecture for a variety of CNN- and transformer-based backbones (see Supplementary Materials

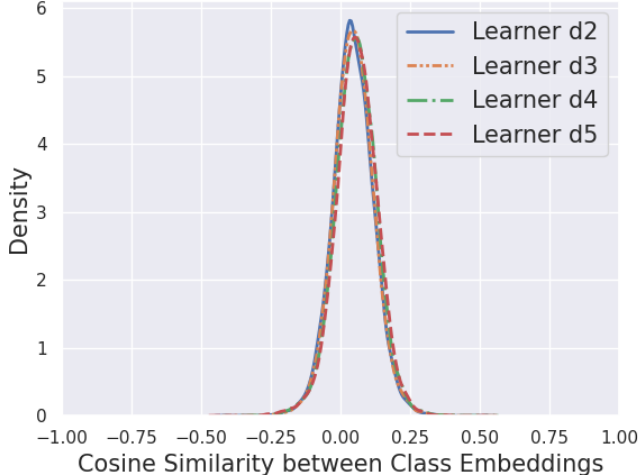


Figure 3. Distribution of the cosine similarity between the different class embeddings for each learner in SenFormer.

for results on additional datasets). As we can see from Table 1, when using the same standard Swin-Transformer backbone, SenFormer consistently outperforms UperNet regardless of the backbone size. The same can be said for the BEiT backbone. In fact, SenFormer outperforms the current state-of-the-art and achieved a new score of 57.05 when a BEiT-L backbone is used. The performance gap is even larger when using convolutional backbones (+3  $mIoU$ ), suggesting that our transformer-based decoder successfully capture the long-range dependencies missed by the CNN-based backbones.

Since SenFormer uses one learner per level in the feature pyramid, it has more parameters than its *features fusion* counterpart. But when compared to traditional ensemble methods that require the training of several independent models, our self-ensemble framework is much more parameter- and computationally efficient as it involves training a single model. Moreover, SenFormer is more efficient than UperNet in terms of FLOPs.

**Class embeddings similarity.** In SenFormer, for a given learner, each class embedding vector represents a unique class and is used to produce the learner’s prediction for that given class. Hence, we expect the class embedding to retain specific information about that class. Accordingly, at the end of the training the different learners should converge to different vectors (as they represent different classes).

Figure 3 shows the distribution density of the cosine similarity between the different class embeddings of SenFormer trained on ADE20K with ResNet-50 as backbone; *i.e.* for the  $i$ -th learner the distribution of the following set  $\{\cos(cls_i^k, cls_i^l), (k, l) \in \{1, \dots, N_c - 1\} \times \{k, \dots, N_c\}\}$ .

Surprisingly, although ADE20K has a large number of classes, the density curves are close to the origin, suggest-

ing that the different class embeddings converge to different vectors. Hence, for a given learner  $i$ , the class embeddings  $\mathbf{cls}_i = [cls_i^1, \dots, cls_i^{N_c}]$  of SenFormer effectively acts as a *memory bank* that is used by the decoder to assess how likely a given feature token of  $P_i$  represents a certain class.

In our experiments when we tried to use a unique class embedding for the different learners, it led to significantly degraded performance, hinting that the different decoders genuinely behave as independent learners. See Supplementary Materials for additional experiments on sharing settings between learners.

#### 4.4. Ablation studies

For ablation studies, we solely use ResNet-50 pre-trained on ImageNet-1K [39] as backbone and trained all models for 100k iterations.

# block	$mIoU$	#params.	FLOPs
1	42.44	55M	111G
3	43.25	89M	139M
6	43.6	144M	179G
9	<b>43.7</b>	190M	220G

(a) Number of decoder blocks.

method	$mIoU$	method	$mIoU$
none	38.15	Post-Norm	42.63
FPN	42.7	Pre-Norm	<b>43.6</b>
FPNT	<b>43.6</b>		

(b) FPN vs FPNT.

(c) Normalization strategy.

Table 4. Ablation studies related to SenFormer architectural choices.

**Number of blocks.** Table 4 show the results of SenFormer trained with varying number of decoder block per learner. The  $mIoU$  improves with more decoder blocks added. Note that using a single decoder block leads to significantly poorer performance, suggesting that cross-correlation are iteratively drawn between the feature  $P_i$ ’s and the class embeddings  $\mathbf{cls}_i$ ’s. We choose to use 6 decoder blocks per learner as it offers a good complexity/performance trade-off.

**FPN/FPNT Multi-scales feature generation.** In Table 4 we demonstrate the benefit of our feature pyramid network transformer (FPNT) over the traditional FPN and its crucial role in our architecture. We observe that FPNT is 0.9  $mIoU$  better than the FPN baseline, while introducing a minimal parameter and computational overhead. Also, not using any FPN-like method significantly reduces the performance, which can be explained by the fact that each learner must receive semantically and spatially strong features.

**Pre-Norm vs Post-Norm.** Early versions of transformers [43] as well as recent applications to object detection

and segmentation [5, 9] applied layer normalization after the skip connection (post-norm), while recent implementations tend toward using pre-normalization setting. Table 4 shows that a pre-normalization strategy performs best for our architecture. We believe that, by leaving the skip connection pathway unaltered, the pre-norm setting ease the information flow from the ground truth supervision to the input class embeddings of the learner, therefore fostering the "memory bank" mechanism described Section 4.3. It may also explain why [5, 9] do not benefit from the use of pre-norm. Indeed, in DETR and MaskFormer, each *query embedding* vector (the equivalent of our class embedding) does not correspond to a unique class, but is rather dynamically routed to a class by using a bipartite matching, therefore the learned embeddings do not act as a "memory bank".

## 5. Conclusion

This paper introduces our self-ensemble framework for semantic segmentation, a simple methodology that benefits from ensemble learning while avoiding the inconvenience and cost of training multiple times the same model. To do so, we proposed to leverage the multi-scale feature set produced by FPN-like methods to build an ensemble of decoders within a *single model*, where learners in the ensemble are fed with features coming from different levels of the feature pyramid. We also developed a transformer-based architecture for the learner/decoders. In addition, we proposed an enhanced version of the traditional FPN that uses transformer blocks in place of convolutions and therefore introducing minimal changes to the implementation while notably improving segmentation performance.

Our approach outperforms current state-of-the-art on ADE20K, Pascal Context and COCO-Stuff-10K datasets for semantic segmentation. It is more efficient in terms of FLOPs, but requires notably more parameters due to the use of multiple decoders/learners. It is part of our future work to investigate light-weight learners and improve efficiency.

## Acknowledgements

We thank Romain Fabre for insightful discussion without which this paper would not be possible. This work was partially supported by the National Institutes of Health (NIH), National Cancer Institute (NCI) Human Tumor Atlas Network (HTAN) Research Center (U2C CA233280), and a NIH/NCI Cancer Systems Biology Consortium Center (U54 CA209988).

## Supplementary Materials

To demonstrate the generality of our self-ensemble framework, we evaluate SenFormer performances on additional benchmark datasets for semantic segmentation with various number of classes and training samples. We first

method	backbone	<i>mIoU</i>	+MS
DeepLabV3+ [8]	ResNet-50	44.0	44.9
PerPixelBaseline+ [9]	ResNet-50	41.9	42.9
MaskFormer [9]	ResNet-50	44.5	46.7
<b>SenFormer</b>	ResNet-50	<b>44.68</b>	45.2
OCRNet [51]	ResNet-101	-	45.3
DeepLabV3+ [8]	ResNet-101	45.5	46.4
MaskFormer [9]	ResNet-101	45.5	47.2
<b>SenFormer</b>	ResNet-101	<b>46.54</b>	47.0
SETR-L MLA [53]	ViT-L	-	50.3
Segmenter [41]	ViT-L	50.71	52.25
Segmenter-Mask [41]	ViT-L	51.82	53.63
SegFormer [49]	MiT-B5	51.0	51.8
UperNet [30]	Swin-L	52.05	53.5
<b>SenFormer</b>	Swin-L	53.08	54.2
MaskFormer [9]	Swin-L	<b>54.1</b>	<b>55.6</b>

Table 5. State-of-the-art comparison on ADE20K validation set.

provide more information about the datasets used to evaluate SenFormer performances (Section A). Then we compare SenFormer to state-of-the-art architectures on these datasets (Section B). Eventually, to gain more insights about our self-ensemble approach, additional experiments and ablations on SenFormer are presented on ADE20K dataset (Section C).

## A. Additional datasets

**ADE20K** [54] is a scene parsing dataset built from ADE20K-Full dataset, where 150 classes were selected to constitute SceneParse150 challenge. It consists of 20,210 training images, 2,000 validation images, and covers 150 fine-grained labeled classes. Models are trained for 160k iterations, with a batch size of 16 and a crop size of  $640 \times 640$  pixels when using Swin-B, Swin-L or BEiT-L as backbone, otherwise a crop size of  $512 \times 512$  is used.

**COCO-Stuff-10K** [4] is a subset of the COCO dataset [29] for semantic segmentation. It consists of 9k images for training and 1k images for testing, covering 171 semantic-level categories. For training, all SenFormer models were trained for 80k iterations, with a batch size of 16 and a crop size of  $512 \times 512$ .

**Pascal Context** [35] training set contains 4,996 images covering 59 classes and the testing set contains 5,104 images. The data come from the PASCAL VOC 2010 contest [14], where annotations for the whole scene have been added. All SenFormer models were trained for 40k iterations, with a batch size of 16 and a crop size of  $480 \times 480$ .

**Cityscapes** [11] is a high-resolution dataset of 5,000



street-view images with 19 semantic classes. Conventionally, the dataset is split into a training set of 2,975 images and a validation set of 500 images. All SenFormer models were trained for 100k iterations, with a batch size of 8 and a crop size of  $512 \times 1024$ .

## B. Additional results

In this section we further compare SenFormer to state-of-the-art methods on ADE20K and additional benchmark datasets.

**ADE20K.** In Table 5 we compare SenFormer to a variety of FCN- and transformer-based decoders using both CNN- and transformer-based backbones. When using standard ResNet backbones, SenFormer outperforms all other methods. The same can be said for per-pixel classification-based models when using transformer-based backbones, where SenFormer even outperforms recently introduced transformer-based decoders like SETR [53], Segmenter [41] and SegFormer [49]. Note however that MaskFormer [9] is doing better than SenFormer when using transformer-based backbones. Indeed, MaskFormer introduces a new approach for semantic segmentation that is based on mask classification (rather than traditional per-pixel classification) and that greatly improves segmentation performances. In fact, MaskFormer [9] significantly outperforms PerPixel-Baseline+ [9] while sharing the same architecture and only differing by the problem formulation (*per-pixel vs mask classification*). Therefore, we leave for the future work SenFormer’s formulation as a mask classification, as it has significant potential for semantic segmentation.

**Pascal Context.** In Table 6 we compare SenFormer to state-of-the-art methods on Pascal Context test dataset. The current state-of-the-art performance is obtained by CAA [21] using EfficientNet-B7 as backbone, with a mIoU of 60.5. SenFormer is outperforming previous FCN methods when using standard ResNet backbones, as well as recent transformer-based methods. Our approach outperforms the current state-of-the-art (CAA) when using the same ResNet-101 backbone, showing the benefit of our approach. Moreover, we reach a score of **64.0** mIoU when using Swin-L as backbone. Overall, our approach shows a significant improvement of +3.5 mIoU over the previous state-of-the-art.

**COCO-Stuff-10K.** Table 7 compares SenFormer to state-of-the-art methods on COCO-Stuff-10K test dataset. The current state-of-the-art performance is obtained by CAA [21] using EfficientNet-B7 as backbone, with a mIoU of 45.4. When using standard ResNet backbones, SenFormer outperforms previous FCN methods, as well as the transformer-based method MaskFormer. Moreover, we obtain **50.1** mIoU when using Swin-L as backbone. Therefore, our approach pushes SOTA’s boundaries by a substantial margin of +4.6 mIoU over previous methods on COCO-

method	backbone	mIoU	+MS
DANet [17]	ResNet-50	-	50.5
EMANet [26]	ResNet-50	-	50.5
CAA [21]	ResNet-50	50.23	-
<b>SenFormer</b>	<b>ResNet-50</b>	<b>53.18</b>	<b>54.3</b>
DANet [17]	ResNet-101	-	52.6
EMANet [26]	ResNet-101	-	53.1
DeepLabV3+ [8]	ResNet-101	53.2	54.67
DRANet [16]	ResNet-101	-	55.4
OCRNet [51]	ResNet-101	-	54.8
CAA [21]	ResNet-101	-	55.0
<b>SenFormer</b>	<b>ResNet-101</b>	<b>55.1</b>	<b>56.6</b>
OCRNet [51]	HRNetV2-W48	-	56.2
CAA [21]	EfficientNet-B7	58.40	60.5 <sup>‡</sup>
SETR-L MLA [53]	ViT-L	54.9	55.8
Segmenter [41]	ViT-L	50.71	56.5
Segmenter-Mask [41]	ViT-L	58.1	59.0
<b>SenFormer</b>	<b>Swin-L</b>	<b>62.4</b>	<b>64.0</b>

Table 6. State-of-the-art comparison on Pascal Context test. <sup>‡</sup> indicates previous SOTA and score in blue indicates the new SOTA

method	backbone	mIoU	+MS
EMANet [26]	ResNet-50	-	37.6
PerPixelBaseline+ [9]	ResNet-50	34.2	35.8
MaskFormer [9]	ResNet-50	37.1	38.9
<b>SenFormer</b>	<b>ResNet-50</b>	<b>39.0</b>	<b>39.7</b>
DANet [17]	ResNet-101	-	39.7
EMANet [26]	ResNet-101	-	39.9
OCRNet [51]	ResNet-101	-	39.5
CAA [21]	ResNet-101	-	41.2
MaskFormer [9]	ResNet-101	38.1	39.8
<b>SenFormer</b>	<b>ResNet-101</b>	<b>39.6</b>	<b>40.6</b>
OCRNet [51]	HRNetV2-W48	-	40.5
CAA [21]	EfficientNet-B7	-	45.4 <sup>‡</sup>
<b>SenFormer</b>	<b>Swin-L</b>	<b>49.1</b>	<b>50.1</b>

Table 7. State-of-the-art comparison on COCO-Stuff-10K test. <sup>‡</sup> indicates previous SOTA and score in blue indicates the new SOTA.

Stuff-10K.

**Cityscapes.** Table 8 compare SenFormer to state-of-the-art methods on Cityscapes validation dataset. We observe that SenFormer performs on par with the best FCN and transformer-based methods. We hypothesis that since Cityscapes dataset has only 19 classes, the object classification aspect of the segmentation is easier and therefore SenFormer cannot benefit as much from its class embed-

method	backbone	<i>mIoU</i>	+MS
MaskFormer [9]	ResNet-50	78.5	-
SenFormer	ResNet-50	78.8	80.1
DeepLabV3+ [8]	ResNet-50	<b>78.97</b>	<b>80.46</b>
MaskFormer [9]	ResNet-101	79.7	81.4
SenFormer	ResNet-101	80.3	81.4
OCRNet [51]	ResNet-101	-	82.0
DeepLabV3+ [8]	ResNet-101	80.9	82.03
SETR-L PUP [53]	ViT-L	-	82.2
Segmenter [41]	ViT-L	-	80.7
Segmenter-Mask [41]	ViT-L	79.1	81.3
SenFormer	Swin-L	82.15	83.3
SegFormer [49]	MiT-B5	82.4	84.0

Table 8. State-of-the-art comparison on Cityscapes validation.

dings/memory banks, as it does with datasets where the number of classes is larger.

### C. Additional experiments

To gain more insights on how SenFormer is making its predictions and how independent the different learners in SenFormer are from each other, we conduct additional experiments. For the following experiments, we use ResNet-50 pretrained on ImageNet-1K as backbone and train all the models for 160K iterations on ADE20K.

**Iterative cross-correlations.** In the ablation studies, we demonstrate that reducing the number of blocks per learner significantly poorer the performance – -1.3 *mIoU* when using a single decoder block compared to using 6. We therefore concluded that cross-correlations are iteratively drawn between the features  $P_i$ 's and the class embeddings  $\mathbf{cls}_i$ 's. To further validate it, we trained a SenFormer variant where each learner is using a single block repeated 6 times – *i.e.*, each learner has 6 weight-shared decoder blocks. As we can see from Table 9, this sharing setting achieves notably better performance than straightforwardly using a single block. Hence, validate our thought on the iterative nature of the knowledge transfer from the features  $P_i$ 's to the embeddings  $\mathbf{cls}_i$ 's. Note also that sharing weights across the blocks allows to dramatically reduce the number of parameters, thus surpasses UperNet [48] with *less parameters* and FLOPs. In [22], the authors observe similar behavior when using the same transformer block several times.

**Weight sharing.** The initial observation of our approach was that the different levels of the feature pyramid carry different amounts of scale and contextual information and that a single decoder/learner cannot take full advantage of all of them. In the experiment section, we have shown that SenFormer performs better than both UperNet and FeaturesFu-

weight sharing setting	# blocks	<i>mIoU</i>	#params.	FLOPs
shared	6	42.69	68M	179G
cls embedding	6	42.91	67M	179G
repeated	6	44.16	<b>55M</b>	179G
none	1	43.12	<b>55M</b>	<b>111G</b>
none	6	<b>44.68</b>	144M	179G
UperNet		42.05	67M	238G

Table 9. Comparison performance on ADE20K val of different weight sharing settings for SenFormer. *shared*: the same decoder is shared for all the level. *cls embedding*: only the class embeddings is share across the learners. *repeated*: each learner/decoder is independent and use a single decoder block repeated 6 times. Last row is UperNet [48] result for comparison purpose.

sionBaseline that use a single decoder.

To further validate our hypothesis, we trained a variant of SenFormer where a single learner/decoder is used to process the different levels of the feature pyramid – *i.e.*, a single decoder is *shared across all the learners*. As we can see from Table 9, this sharing setting leads to significantly poorer performance, thus supporting our assumption.

To further verify that independence between learners is a key component in SenFormer, we trained another variant of SenFormer where the learners/decoders are distinct but use the same class embeddings – *i.e.*,  $\mathbf{cls}_2 = \mathbf{cls}_3 = \mathbf{cls}_4 = \mathbf{cls}_5$ . Table 9 shows that sharing the class embeddings also leads to a significant degradation in performances, hinting that the different decoders genuinely behave as independent learners.

In summary, the process during which the knowledge contained in the features is distilled into the class embeddings, is an iterative process, therefore requires several decoder blocks (may their weights be shared or not). Moreover, independence between SenFormer's learners is a key requirement of our approach, hence any weight sharing between the learners will significantly poorer performances.

### References

- [1] Berat Mert Albaba and Sedat Ozer. Synet: An ensemble network for object detection in uav images, 2020. 2
- [2] Zeyuan Allen-Zhu and Yuanzhi Li. Towards understanding ensemble, knowledge distillation and self-distillation in deep learning, 2021. 2, 5
- [3] Hangbo Bao, Li Dong, and Furu Wei. Beit: Bert pre-training of image transformers, 2021. 2, 5, 6
- [4] Holger Caesar, Jasper Uijlings, and Vittorio Ferrari. Coco-stuff: Thing and stuff classes in context, 2018. 5, 8

- [5] Nicolas Carion, Francisco Massa, Gabriel Synnaeve, Nicolas Usunier, Alexander Kirillov, and Sergey Zagoruyko. End-to-end object detection with transformers, 2020. **2, 5, 8**
- [6] Liang-Chieh Chen, George Papandreou, Iasonas Kokkinos, Kevin Murphy, and Alan L. Yuille. Deeplab: Semantic image segmentation with deep convolutional nets, atrous convolution, and fully connected crfs, 2017. **1, 2, 5**
- [7] Liang-Chieh Chen, George Papandreou, Florian Schroff, and Hartwig Adam. Rethinking atrous convolution for semantic image segmentation, 2017. **1, 2**
- [8] Liang-Chieh Chen, Yukun Zhu, George Papandreou, Florian Schroff, and Hartwig Adam. Encoder-decoder with atrous separable convolution for semantic image segmentation. In *Proceedings of the European conference on computer vision (ECCV)*, pages 801–818, 2018. **8, 9, 10**
- [9] Bowen Cheng, Alexander G. Schwing, and Alexander Kirillov. Per-pixel classification is not all you need for semantic segmentation, 2021. **1, 2, 5, 8, 9, 10**
- [10] MMSegmentation Contributors. MMSegmentation: Openmmlab semantic segmentation toolbox and benchmark. <https://github.com/open-mmlab/mms Segmentation>, 2020. **5**
- [11] Marius Cordts, Mohamed Omran, Sebastian Ramos, Timo Rehfeld, Markus Enzweiler, Rodrigo Benenson, Uwe Franke, Stefan Roth, and Bernt Schiele. The cityscapes dataset for semantic urban scene understanding, 2016. **5, 8**
- [12] Alexey Dosovitskiy, Lucas Beyer, Alexander Kolesnikov, Dirk Weissenborn, Xiaohua Zhai, Thomas Unterthiner, Mostafa Dehghani, Matthias Minderer, Georg Heigold, Sylvain Gelly, Jakob Uszkoreit, and Neil Houlsby. An image is worth 16x16 words: Transformers for image recognition at scale, 2021. **1, 2**
- [13] Alaaeldin El-Nouby, Hugo Touvron, Mathilde Caron, Piotr Bojanowski, Matthijs Douze, Armand Joulin, Ivan Laptev, Natalia Neverova, Gabriel Synnaeve, Jakob Verbeek, and Hervé Jegou. Xcit: Cross-covariance image transformers, 2021. **1, 2**
- [14] Mark Everingham, Luc Van Gool, Christopher K. I. Williams, John M. Winn, and Andrew Zisserman. The pascal visual object classes (voc) challenge. *International Journal of Computer Vision*, 88:303–338, 2009. **8**
- [15] Stanislav Fort, Huiyi Hu, and Balaji Lakshminarayanan. Deep ensembles: A loss landscape perspective, 2020. **2**
- [16] Jun Fu, Jing Liu, Jie Jiang, Yong Li, Yongjun Bao, and Hanqing Lu. Scene segmentation with dual relation-aware attention network. *IEEE Transactions on Neural Networks and Learning Systems*, 32(6):2547–2560, 2021. **9**
- [17] Jun Fu, Jing Liu, Haijie Tian, Yong Li, Yongjun Bao, Zhiwei Fang, and Hanqing Lu. Dual attention network for scene segmentation. In *Proceedings of the IEEE/CVF Conference on Computer Vision and Pattern Recognition*, pages 3146–3154, 2019. **9**
- [18] Kaiming He, Xiangyu Zhang, Shaoqing Ren, and Jian Sun. Deep residual learning for image recognition, 2015. **3, 5**
- [19] Mohammad Hesam Hesamian, Wenjing Jia, Xiangjian He, and Paul J. Kennedy. Deep learning techniques for medical image segmentation: Achievements and challenges. *Journal of Digital Imaging*, 32:582 – 596, 2019. **1**
- [20] Zhang-Wei Hong, Chen Yu-Ming, Shih-Yang Su, Tzu-Yun Shann, Yi-Hsiang Chang, Hsuan-Kung Yang, Brian Hsi-Lin Ho, Chih-Chieh Tu, Yueh-Chuan Chang, Tsu-Ching Hsiao, Hsin-Wei Hsiao, Sih-Pin Lai, and Chun-Yi Lee. Virtual-to-real: Learning to control in visual semantic segmentation, 2018. **1**
- [21] Ye Huang, Di Kang, Wenjing Jia, Xiangjian He, and Liu Liu. Channelized axial attention for semantic segmentation – considering channel relation within spatial attention for semantic segmentation, 2021. **9**
- [22] Andrew Jaegle, Felix Gimeno, Andrew Brock, Andrew Zisserman, Oriol Vinyals, and Joao Carreira. Perceiver: General perception with iterative attention, 2021. **10**
- [23] Wonsik Kim, Bhavya Goyal, Kunal Chawla, Jungmin Lee, and Keunjoo Kwon. Attention-based ensemble for deep metric learning, 2018. **2**
- [24] Balaji Lakshminarayanan, Alexander Pritzel, and Charles Blundell. Simple and scalable predictive uncertainty estimation using deep ensembles, 2017. **2**
- [25] Stefan Lee, Senthil Purushwalkam, Michael Cogswell, David Crandall, and Dhruv Batra. Why m heads are better than one: Training a diverse ensemble of deep networks, 2015. **2**
- [26] Xia Li, Zhisheng Zhong, Jianlong Wu, Yibo Yang, Zhouchen Lin, and Hong Liu. Expectation-maximization attention networks for semantic segmentation. In *Proceedings of the IEEE/CVF International Conference on Computer Vision*, pages 9167–9176, 2019. **9**
- [27] Tsung-Yi Lin, Piotr Dollár, Ross Girshick, Kaiming He, Bharath Hariharan, and Serge Belongie. Feature pyramid networks for object detection, 2017. **1, 3**
- [28] Tsung-Yi Lin, Priya Goyal, Ross Girshick, Kaiming He, and Piotr Dollár. Focal loss for dense object detection, 2018. **4**
- [29] Tsung-Yi Lin, Michael Maire, Serge Belongie, Lubomir Bourdev, Ross Girshick, James Hays, Pietro Perona, Deva Ramanan, C. Lawrence Zitnick, and Piotr Dollár. Microsoft coco: Common objects in context, 2015. **8**
- [30] Ze Liu, Yutong Lin, Yue Cao, Han Hu, Yixuan Wei, Zheng Zhang, Stephen Lin, and Baining Guo. Swin transformer: Hierarchical vision transformer using shifted windows, 2021. **1, 2, 3, 5, 8**
- [31] Jonathan Long, Evan Shelhamer, and Trevor Darrell. Fully convolutional networks for semantic segmentation. *CoRR*, abs/1411.4038, 2014. **1, 2**
- [32] Ilya Loshchilov and Frank Hutter. Decoupled weight decay regularization, 2019. **5**
- [33] Vladimir Macko, Charles Weill, Hanna Mazzawi, and Javier Gonzalez. Improving neural architecture search image classifiers via ensemble learning, 2019. **2**
- [34] Dimitris Marmanis, Jermaine Wegner, Silvano Galliani, Konrad Schindler, Mihai Datcu, and Uwe Stilla. Semantic segmentation of aerial images with an ensemble of cnns. *ISPRS Annals of Photogrammetry, Remote Sensing and Spatial Information Sciences*, III-3:473–480, 06 2016. **2**

- [35] Roozbeh Mottaghi, Xianjie Chen, Xiaobai Liu, Nam-Gyu Cho, Seong-Whan Lee, Sanja Fidler, Raquel Urtasun, and Alan Yuille. The role of context for object detection and semantic segmentation in the wild. In *2014 IEEE Conference on Computer Vision and Pattern Recognition*, pages 891–898, 2014. [5](#), [8](#)
- [36] Toan Q Nguyen and Julian Salazar. Transformers without tears: Improving the normalization of self-attention. *arXiv preprint arXiv:1910.05895*, 2019. [3](#)
- [37] Ishan Nigam, Chen Huang, and Deva Ramanan. Ensemble knowledge transfer for semantic segmentation. *2018 IEEE Winter Conference on Applications of Computer Vision (WACV)*, pages 1499–1508, 2018. [2](#)
- [38] Olaf Ronneberger, Philipp Fischer, and Thomas Brox. U-net: Convolutional networks for biomedical image segmentation. In *International Conference on Medical image computing and computer-assisted intervention*, pages 234–241. Springer, 2015. [1](#)
- [39] Olga Russakovsky, Jia Deng, Hao Su, Jonathan Krause, Sanjeev Satheesh, Sean Ma, Zhiheng Huang, Andrej Karpathy, Aditya Khosla, Michael Bernstein, Alexander C. Berg, and Li Fei-Fei. Imagenet large scale visual recognition challenge, 2015. [6](#), [7](#)
- [40] Mennatullah Siam, Sara Elkerdawy, Martin Jagersand, and Senthil Yogamani. Deep semantic segmentation for automated driving: Taxonomy, roadmap and challenges, 2017. [1](#)
- [41] Robin Strudel, Ricardo Garcia, Ivan Laptev, and Cordelia Schmid. Segformer: Transformer for semantic segmentation, 2021. [1](#), [2](#), [8](#), [9](#), [10](#)
- [42] Hugo Touvron, Matthieu Cord, Matthijs Douze, Francisco Massa, Alexandre Sablayrolles, and Hervé Jégou. Training data-efficient image transformers & distillation through attention, 2021. [1](#), [2](#)
- [43] Ashish Vaswani, Noam Shazeer, Niki Parmar, Jakob Uszkoreit, Llion Jones, Aidan N. Gomez, Lukasz Kaiser, and Illia Polosukhin. Attention is all you need, 2017. [2](#), [3](#), [7](#)
- [44] Huiyu Wang, Yukun Zhu, Hartwig Adam, Alan Yuille, and Liang-Chieh Chen. Max-deeplab: End-to-end panoptic segmentation with mask transformers, 2021. [1](#), [2](#)
- [45] Wenhai Wang, Enze Xie, Xiang Li, Deng-Ping Fan, Kaitao Song, Ding Liang, Tong Lu, Ping Luo, and Ling Shao. Pyramid vision transformer: A versatile backbone for dense prediction without convolutions, 2021. [1](#), [2](#)
- [46] Wenxiao Wang, Lu Yao, Long Chen, Binbin Lin, Deng Cai, Xiaofei He, and Wei Liu. Crossformer: A versatile vision transformer hinging on cross-scale attention, 2021. [1](#), [2](#)
- [47] Pan Wei, John E. Ball, and Derek T. Anderson. Fusion of an ensemble of augmented image detectors for robust object detection, 2018. [2](#)
- [48] Tete Xiao, Yingcheng Liu, Bolei Zhou, Yuning Jiang, and Jian Sun. Unified perceptual parsing for scene understanding, 2018. [1](#), [2](#), [3](#), [5](#), [6](#), [10](#)
- [49] Enze Xie, Wenhai Wang, Zhiding Yu, Anima Anandkumar, Jose M. Alvarez, and Ping Luo. Segformer: Simple and efficient design for semantic segmentation with transformers, 2021. [1](#), [2](#), [8](#), [9](#), [10](#)
- [50] Steven Young, Tamer Abdou, and Ayse Basar Bener. Deep super learner: A deep ensemble for classification problems. *ArXiv*, abs/1803.02323, 2018. [2](#)
- [51] Yuhui Yuan, Xiaokang Chen, Xilin Chen, and Jingdong Wang. Segmentation transformer: Object-contextual representations for semantic segmentation, 2021. [8](#), [9](#), [10](#)
- [52] Hengshuang Zhao, Jianping Shi, Xiaojuan Qi, Xiaogang Wang, and Jiaya Jia. Pyramid scene parsing network, 2017. [2](#)
- [53] Sixiao Zheng, Jiachen Lu, Hengshuang Zhao, Xiatian Zhu, Zekun Luo, Yabiao Wang, Yanwei Fu, Jianfeng Feng, Tao Xiang, Philip H. S. Torr, and Li Zhang. Rethinking semantic segmentation from a sequence-to-sequence perspective with transformers, 2021. [1](#), [2](#), [8](#), [9](#), [10](#)
- [54] Bolei Zhou, Hang Zhao, Xavier Puig, Tete Xiao, Sanja Fidler, Adela Barriuso, and Antonio Torralba. Semantic understanding of scenes through the ade20k dataset, 2018. [2](#), [5](#), [8](#)
- [55] Zhi-Hua Zhou. *Ensemble methods: foundations and algorithms*. Chapman and Hall/CRC, 2019. [2](#)